ZONES OF INFORMATION IN THE AVIRIS SPECTRA

PAUL J. CURRAN, NASA/Ames Research Center, Moffett Field, CA 94035, USA; JENNIFER L. DUNGAN, TGS Technology Inc., NASA/Ames Research Center, Moffett Field, CA 94035, USA.

ABSTRACT

To make the best use of Airborne Visible/Infrared Imaging Spectrometer (AVIRIS) data an investigator needs to know the ratio of signal to random variability or 'noise' (S/N ratio). The signal is land-cover dependent and decreases with both wavelength and atmospheric absorption and random noise comprises sensor noise and intra-pixel variability. The three existing methods for estimating the S/N ratio are inadequate as typical 'laboratory' methods inflate, while 'dark current' and 'image' methods deflate the S/N ratio.

We propose a new procedure called the 'geostatistical' method. It is based on the removal of periodic noise by 'notch filtering' in the frequency domain and the isolation of sensor noise and intra-pixel variability using the semi-variogram. This procedure was applied easily and successfully to five sets of AVIRIS data from the 1987 flying season.

INTRODUCTION

To optimize the use of Airborne Visible/Infrared Imaging Spectrometer (AVIRIS) data there is a need to know the random variability or 'noise' associated with the sensor's signal. This information is required by the user community, as spectral zones of high and low noise will be common to each land-cover and by every investigator, as noise determines the accuracy with which absorption features can be distinguished in the spectra and objects can be detected on the ground. Noise alone is not a very useful measure, as a given level of noise will have a more deleterious effect on data quality if the signal is low. Therefore, the signal to noise, (S/N) ratio, which can be estimated by the ratio of the signal's mean ($\bar{x}$) to its standard deviation (s), will be used here.

The major part of the noise in the AVIRIS signal is additive to the signal and the signal decreases sharply with both an increase in wavelength and atmospheric absorption. Consequently, plots of S/N ratio versus wavelength will be similar in form to signal versus wavelength for each land-cover under investigation.

The aim of the work reported here was to develop a procedure for estimating the per-waveband S/N ratio of AVIRIS data.

ESTIMATING THE S/N RATIO OF AVIRIS DATA

AVIRIS data contain periodic (coherent) sensor noise, that can be removed and random noise that cannot. The noise of relevance to the investigator is random noise: the random sensor noise, which is image independent and intra-pixel variability, which is a result of spatially heterogeneous pixel contents and is image dependent. Unfortunately, methods commonly used to estimate the S/N ratio of remotely sensed imagery (termed for convenience 'laboratory,' 'dark current' and 'image') do not isolate this random noise for the investigator (Table 1).

Table 1. Existing methods for estimating the S/N ratio of AVIRIS data showing the level of signal and type of noise to be estimated. As an investigator's spectra can be free of periodic noise and inter-pixel variability a S/N ratio is required that contains only random sensor noise and intra-pixel variability. Therefore, these three methods either underestimate or overestimate the S/N ratio required by the investigator.

| Method | Signal level | Type of noise | | | | Estimated S/N ratio in relation to that required by investigator | Two examples from these proceedings |
| | | Periodic | Random | | | | |
		Sensor noise	Sensor noise	Intra-pixel varia-bility	Inter-pixel varia-bility		
'Laboratory'	Artificially high	x	x			Higher	Vane Porter
'Dark current'	Natural	x	x	x		Lower	Abrams and Carerre Vane and Green
'Image'	Natural	x	x	x	x	Lower	Conel et al. Clark

A typical 'laboratory, method uses the $\bar{x}$ and s of a homogeneous surface with a high (e.g., 50%) albedo to estimate the S/N ratio for only a few wavebands. The presence of periodic noise will decrease the measured S/N ratio below that required by the investigator (see above) but this is more than compensated by the omission of intra-pixel variability and more importantly, by the use of an artificially high signal. A typical 'dark current' method uses variation (e.g., s) in the signal dark currents as a measure of noise. This value includes periodic noise which deflates the S/N ratio below that required by the investigator. A typical 'image' method uses the $\bar{x}$ and s of four, or more, visually homogeneous pixels as an estimate of the S/N ratio. The

resultant value is deflated below that required by the investigator, for it includes periodic noise (this could have been removed) and inter-pixel variability, which even on a visually homogeneous area can be around 2% of $\bar{x}$ (Conel et al., 1987).

To estimate the S/N ratio of the investigator's data a new procedure is proposed and this we have termed the 'geostatistical' method.

THE 'GEOSTATISTICAL' METHOD FOR ESTIMATING THE S/N RATIO

Following the removal of periodic noise there is a need to estimate random noise, free of inter-pixel variability (Table 1). We therefore require an estimate of variability at a pixel and a tool to do this is the semi-variogram (Curran, 1988). This is produced from a transect of pixels where the radiance z, at pixel number x along the transect has been extracted at regular intervals and where x = 1, 2, ..., n. The relation between a pair of pixels, h intervals apart (the lag distance) can be given by the variance of the differences between all such pairs. This value, the semi-variance y(h), for pixels at distance h apart is given by half the expectation E of their squared difference,

$$y(h) = 1/2 \ E[z(x_i) - z(x_i + h)]^2 .\tag{1}$$

Within the transect there will be m pairs of observations separated by the same lag, this is estimated by,

$$\bar{S}^2 = 1/2m \sum_{i=1}^{m} [z(x_i) - z(x_i + h)]^2 .\tag{2}$$

$\bar{S}^2$ is an unbiased estimate of the semi-variance, y(h), in the population (Webster, 1985) and is a useful measure of the difference between spatially separate pixels (Jupp et al., 1988). The larger $\bar{S}^2$ is and therefore y(h), the less similar the pixels will be. The semi-variogram is a plot of the function that relates semi-variance to lag (Fig. 1) and is described in Webster (1985) and Curran (1988). Three aspects of the semi-variogram are of interest here: (s) sill, the asymptotic upperbound value of y(h); (Co) nugget variance, the limit of y(h) when h approaches 0 and (C) spatially dependent structural variance, the sill minus nugget variance. By definition y(h)=0 when h=0 (Journal and Huijbregts, 1978), in practice however the limit of y(h) when h approaches 0 is positive because the nugget variance represents variability at scales smaller than a pixel.

The nugget variance is a sound estimate of spatially independent image noise at the scale of a pixel as it comprises random sensor noise and intra-pixel variability. The square root of this variance can be used to estimate the standard deviation of the random noise and thereby the S/N ratio of AVIRIS data,

$$\text{S/N ratio} \simeq \bar{x}/\sqrt{Co} .\tag{3}$$

The assumptions underlying the use of nugget variance as an estimate of random noise are summarized in Table 2.
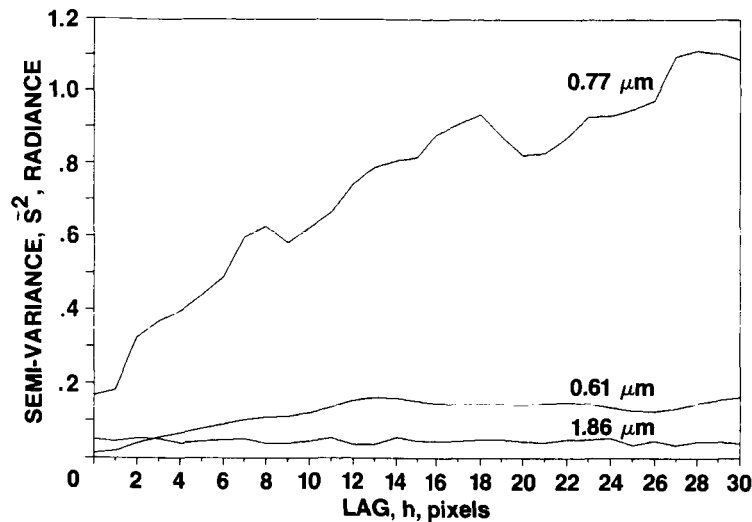
38

Fig. 1. Semi-variograms for three wavebands of AVIRIS data recorded for a plantation forest near Gainesville, Florida (Table 3).

Table 2. Assumptions in the use of nugget variance as an estimate of random noise (random sensor noise and intra-pixel variability) in AVIRIS data.

Assumption	Explanation or reason	Comments on assumptions in relation to AVIRIS data
Stationarity	Spatial dependence of pixels is a function of lag and not location.	Generally true within a land cover.
Isotropy	Nugget variance is independent of transect direction.	Untrue, due to gain and offset variability therefore use row or column transects.
Fixed spatial resolution	Intra-pixel variability and therefore nugget variance is dependent upon spatial resolution.	True.
Scene does not contain random information.	Random features in scene increase nugget variance and could contain information.	Generally true but need to check.
Nugget variance is independent of spatially dependent structural variance.	Limit of y(h) when h approaches 0 has minor dependence upon the slope of the semi-variogram.	Untrue, but point-spread-function of sensor ensures that y(h) when h approaches 0 is similar to that at small lags and so the effect of this violation is minimal.

THE 'GEOSTATISTICAL' METHOD FOR ESTIMATING THE S/N RATIO OF AVIRIS DATA

Application of the 'geostatistical' method involved two stages, first, data selection and preprocessing and second, estimation of the S/N ratio for each waveband of AVIRIS data.

Selection and preprocessing of AVIRIS data

Five AVIRIS data sets were selected (Table 3). They were recorded around solar noon, over a wide range of dates and land-covers. All data were converted from grey levels to radiance and radiometrically calibrated at JPL (Vane et al., 1987) and on receipt dropped scan lines were replaced with the means of adjacent lines.

Table 3. AVIRIS data for which the S/N ratio was estimated.

Location	Land-cover of interest	Date of data acquisition (1987)	Time of data acquisition (start, hrs.)
Mountain View, California	Sediment-laden water	25 June	12:40
Gainesville, Florida	Plantation forest	4 July	11:49
Yuba City, California	Bare soil	30 July	12:49
Metolius, Oregon	Semi-natural forest	1 August	11:14
Cuprite, Nevada	Bare soil	14 September	11:14

The 1987 AVIRIS data contained considerable periodic noise, produced by the inadvertent coupling of the image signal with electrical and mechanical signals. This noise was dominated by frequencies around two pixels per cycle and increased in severity as the season progressed (Fig. 2). The major periodic noise frequencies were removed by 'notch filtering' in the frequency domain of the image (similar to Hlavka, 1986) (Table 4, for method). By comparison with prefiltered spectra this removal of major periodic noise made no difference to the relative radiometry and by comparison with prefiltered semi-variograms it reduced considerably the spatially dependent structural variance (C). The visual effects of such filtering are illustrated in Figs. 3 to 7 for the waveband centered at 1.018 μm. The success of this preprocessing was attributed to: (i) clarity of the noise, especially from 0.68 to 1.27μm (a result of low gain) and 1.84-2.40 μm (a result of low signal); (ii) clarity of the major periodic noise spikes in the vertical component of the frequency domain; (iii) spectrometer-independence of the major periodic noise frequencies and (iv) relatively homogeneous

sub-scenes with little chance of 'ringing' (crenulated tonal boundaries) in the filtered images (Moik, 1980).
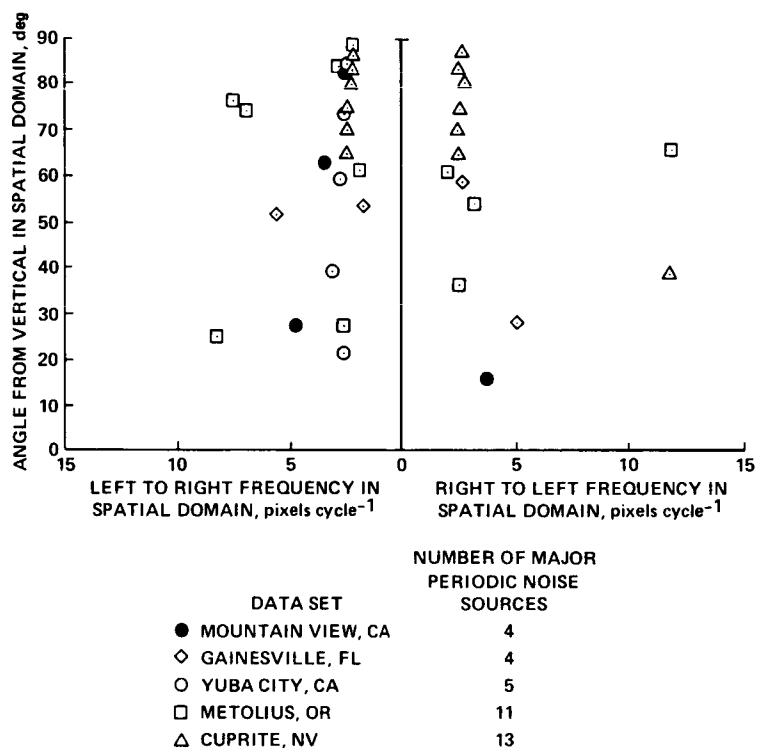

Fig. 2. The major types of periodic noise observed in five sets of AVIRIS data (Table 3). The noise characteristics were determined from the location of major periodic noise spikes in the frequency domain.

Table 4. Removing the major periodic noise in AVIRIS data.

Stage	Procedure
1	Select 256 x 256 pixel sub-scene in one waveband.
2	Use fast Fourier transform to create a frequency domain image; major periodic noise appears as a series of spikes, each representing energy concentration at a specific frequency.
3	Design a 'notch filter', 0's represent the location of major periodic noise spikes and 1's represent the remainder; multiply by frequency domain image to create a new frequency domain image without major periodic noise spikes.
4	Invert filtered frequency domain image to create spatial domain image with no major periodic noise.
5	Repeat 4 on selected wavebands from each spectrometer. Define spectrometer-independent notch filter and use to filter all AVIRIS wavebands.

41

Estimating the S/N ratio for each waveband of AVIRIS data

The procedure for estimating the S/N ratio for each waveband of AVIRIS data is given in Table 5 and the results in Figs. 3 to 7. As was noted in the introduction, noise varies little with wavelength but the signal drops sharply with both an increase in wavelength and atmospheric absorption. As a result the first-order forms of the S/N ratio plots (Figs. 3 to 7) were signal dependent. The spectral zones of very high S/N ratio were green/red (0.50-0.70μm) for water and soil and near infrared (0.95-1.10μm) for vegetation. The spectral zones of high S/N ratio were blue for water and soil (0.40-0.50μm), green/red (0.50-0.70μm) for vegetation and near infrared (0.85-0.90, 0.95-1.10μm) for vegetation and soil respectively. The spectral zones of medium S/N ratio were blue (0.40-0.50μm) for vegetation and the near infrared regions (0.70-0.85μm) for water and vegetation, (0.85-0.95μm) for water and soil, (0.90-0.95μm) for vegetation and (0.95-1.10μm) for water. The regions of low and very low S/N ratio were near and middle infrared wavelengths in zones of low signal, either at long wavelengths or in atmospheric absorption bands. These spectral zones of S/N ratio are a useful summary of the utility of specific AVIRIS wavelengths from the 1987 flight season. Of more importance is the potential use of the 'geostatistical' method by individual investigators to plan for the restrictions that random noise places on the analysis of AVIRIS data.
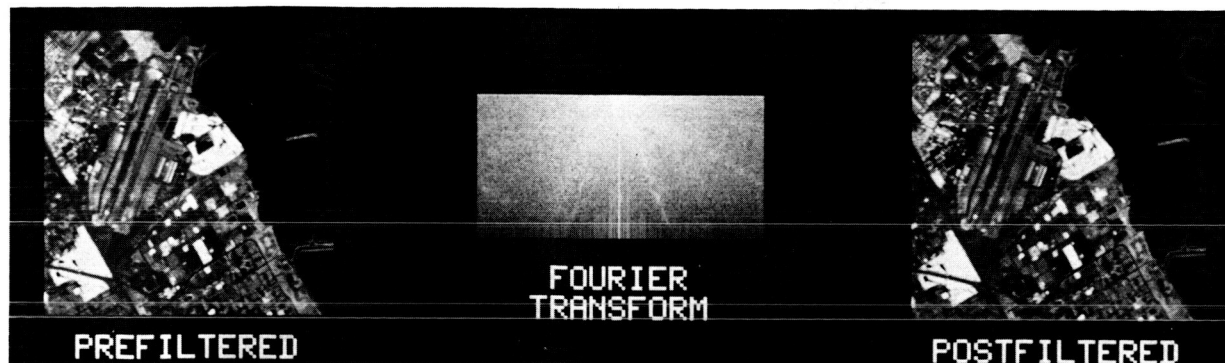
Table 5. Estimating the S/N ratio in AVIRIS data.

Stage	Procedure
1	Locate three row transects within a land-cover, each transect 75-100 pixels long to ensure that the statistically significant first fifth of the semi-variogram is at least 15 lags.
2	Calculate the mean signal ($\bar{x}$) and semi-variogram for each waveband.
3	Determine the nugget variance (Co) by extrapolating the slope of $y(h)/h$ for each waveband. (Here the extrapolation was based on a linear fit over 8 lags, Fig. 1).
4	Plot $\bar{x}/\sqrt{Co}$ versus wavelength and $\bar{x}$ (with a $\sqrt{Co}$ envelope) versus wavelength as two representations of the S/N ratio (Figs. 3 to 7).

CONCLUSIONS

A new prodedure, that we have called the 'geostatistical' method, was used to estimate the S/N ratio of five sets of AVIRIS data. This method was designed around the needs of the AVIRIS investigator and has the following advantages: (i) it estimates only noise that is relevant to the investigator, unlike the existing 'laboratory,' 'dark current' and 'image' methods, (ii) it requires acceptable assumptions and (iii) is easy to apply.

Removal of major periodic noise
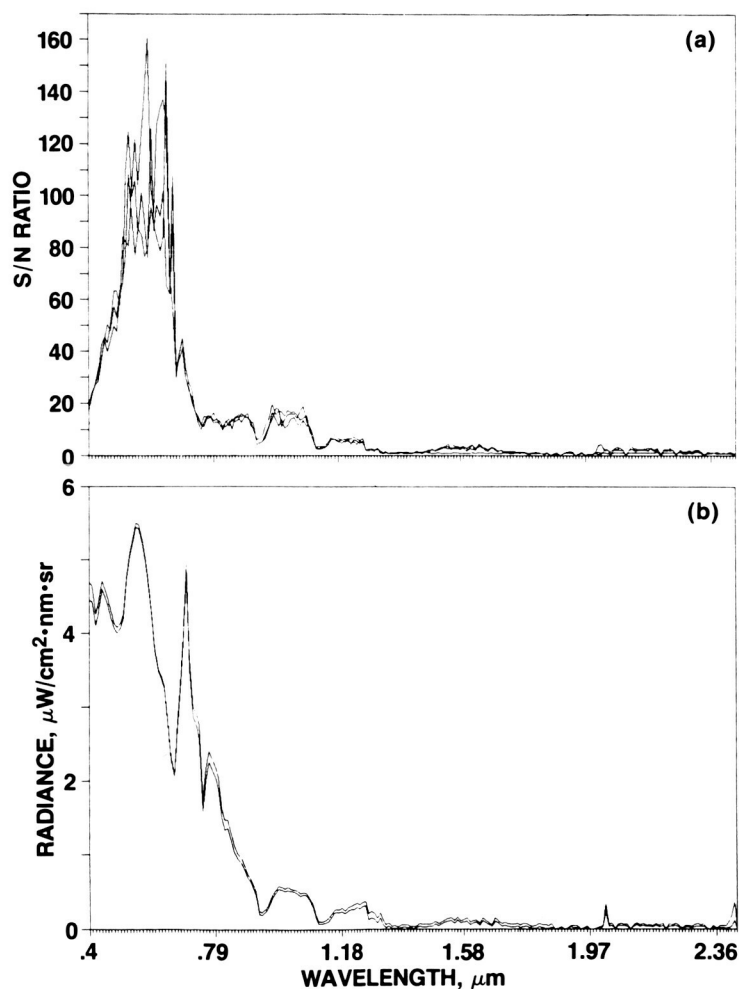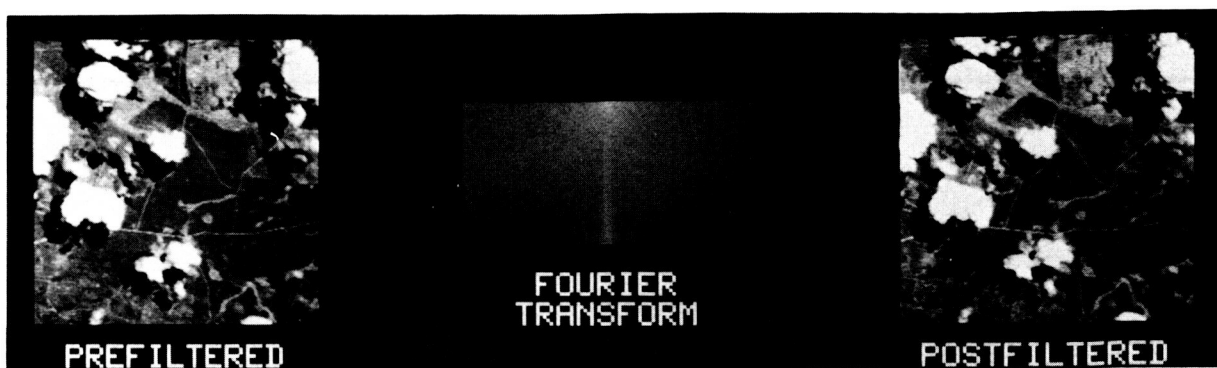

Representations of the S/N ratio

Fig. 3. Estimating the S/N ratio for sediment-laden water in the AVIRIS data of Mountain View, California (Table 3). Above: removal of major periodic noise by 'notch filtering' in the frequency domain. Below: (a) the S/N ratio versus wavelength and (b) the signal, with noise envelope, versus wavelength for three image transects.
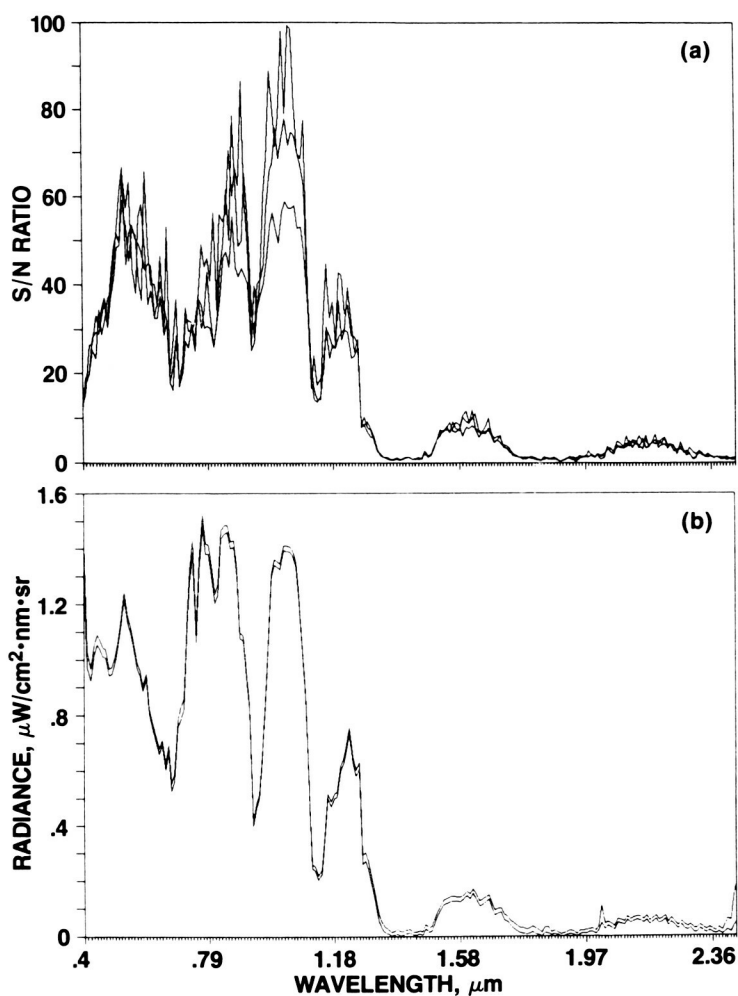
PREFILTERED · FOURIER TRANSFORM · POSTFILTERED

Representations of the S/N ratio

Fig. 4. Estimating the S/N ratio for a plantation forest in the AVIRIS data of Gainesville, Florida (Table 3). Above: removal of major periodic noise by 'notch filtering' in the frequency domain. Below: (a) the S/N ratio versus wavelength and (b) the signal, with noise envelope, versus wavelength for three image transects.

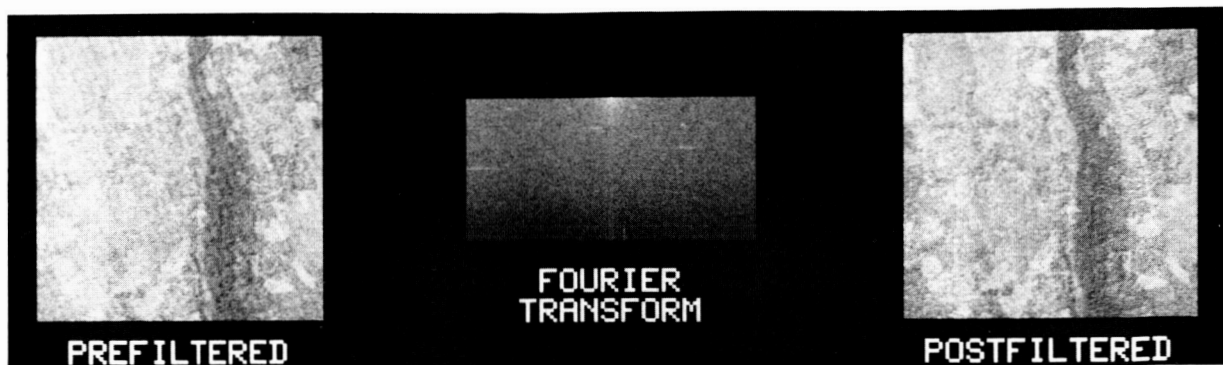Removal of major periodic noise
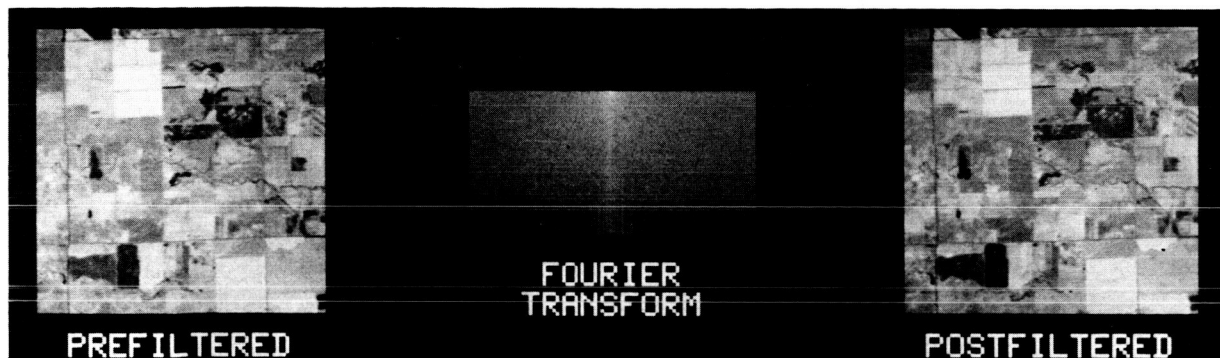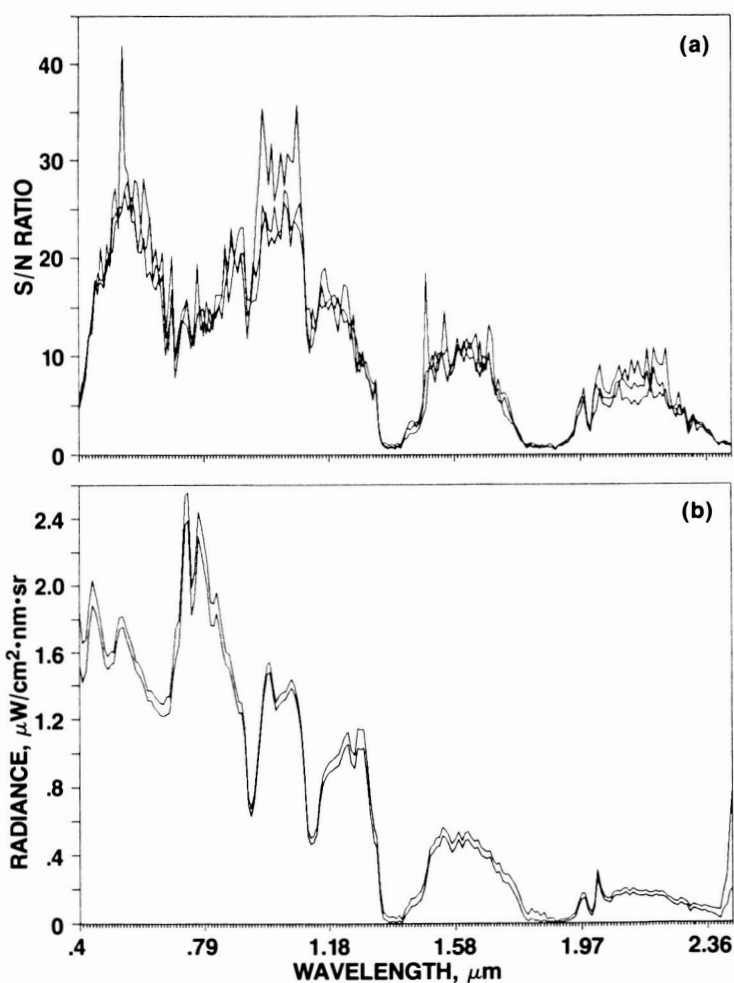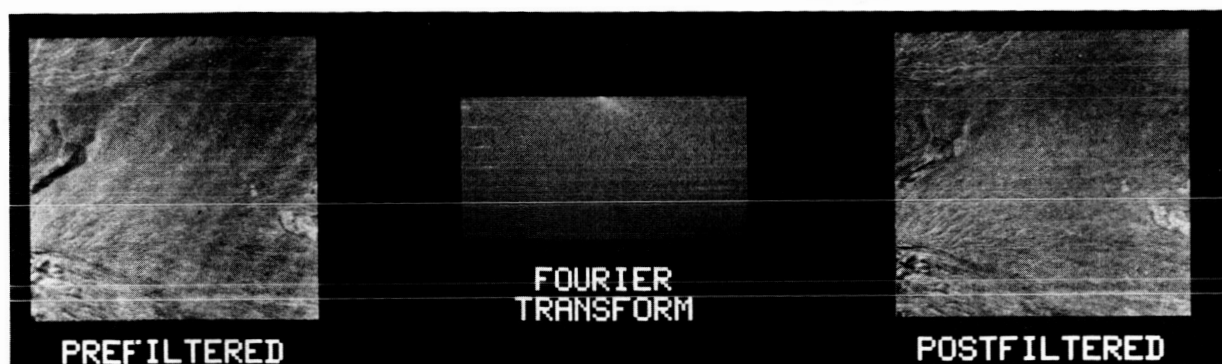

Representations of the S/N ratio
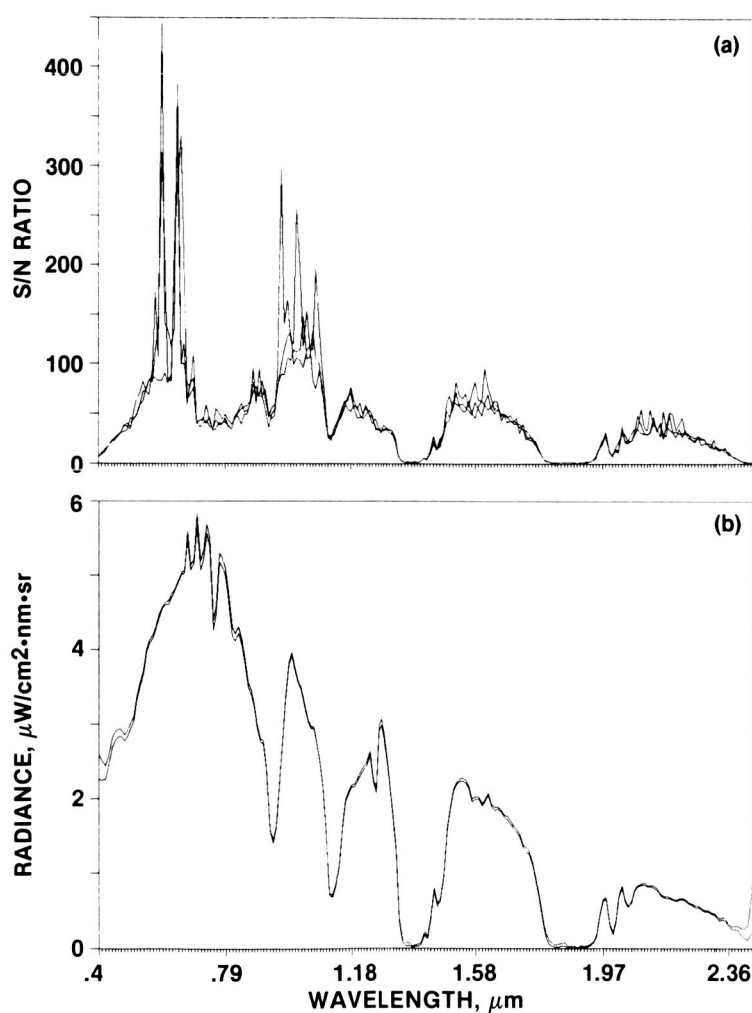
Fig. 5. Estimating the S/N ratio for bare soil in the AVIRIS data of Yuba City, California (Table 3). Above: removal of major periodic noise by 'notch filtering' in the frequency domain. Below: (a) the S/N ratio versus wavelength and (b) the signal, with noise envelope, versus wavelength for three image transects.

Removal of major periodic noise

PREFILTERED   FOURIER TRANSFORM   POSTFILTERED

Representations of the S/N ratio

Fig. 6. Estimating the S/N ratio for semi-natural forest in the AVIRIS data of Metolius, Oregon (Table 3). Above: removal of major periodic noise by 'notch filtering' in the frequency domain. Below: (a) the S/N ratio versus wavelength and (b) the signal, with noise envelope versus wavelength for three image transects.

46

Removal of major periodic noise

PREFILTERED   FOURIER TRANSFORM   POSTFILTERED
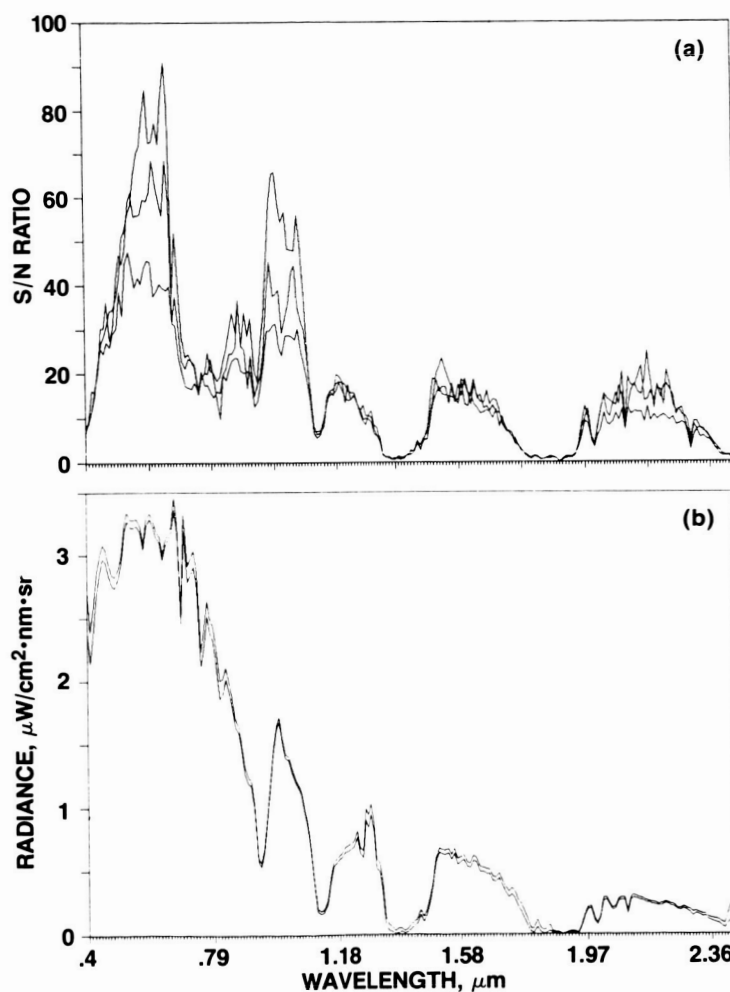
Representations of the S/N ratio

Fig. 7. Estimating the S/N ratio for bare soil in the AVlRIS data of Cuprite, Nevada (Table 3). Above: removal of major periodic noise by 'notch filtering' a fast Fourier transform. Below: (a) the S/N ratio versus wavelength and (b) the signal, with noise envelope, versus wavelength for three image transects.

REFERENCES

Conel, J.E., Green, R.O., Vane, G., Bruegge, C.J., Alley, R.E. and Curtiss, B.J. 1987. Airborne Imaging Spectrometer-2: radiometric spectral characteristics and comparison of ways to compensate for the atmosphere. In Imaging Spectrometry II (G. Vane ed.). SPIE Proceedings 834. Society of Photo-Optical Instrumentation Engineers, Bellingham, Washington: 140-157.

Curran, P.J. 1988. The semivariogram in remote sensing: an introduction. Remote Sensing of Environment, 24: 493-507.

Hlavka, C. 1986. Destriping AIS data using Fourier filtering techniques. In Proceedings of the Second Airborne Spectrometer Data Analysis Workshop (G. Vane and A.F.H. Goetz eds). JPL Publication 86-35. Jet Propulsion Laboratory, Pasadena: 74-80.

Journel, A.G. and Huijbregts, C.J. 1978. Mining Geostatistics. Academic Press, London.

Jupp, D.L.B., Strahler, A.H. and Woodcock, C.E. 1988. Autocorrelation and regularization in digital images. I Basic theory. IEEE Transactions on Geoscience and Remote Sensing, 26: 463-473.

Moik, J.G. 1980. Digital Processing of Remotely Sensed Images. NASA SP-431. National Aeronautics and Space Administration, Washington DC.

Vane, G., Chrien, T.G., Miller, E.A. and Reimer, J.H. 1987. Spectral and radiometric calibration of the Airborne Visible/Infrared Imaging Spectrometer. In Imaging Spectrometry II (G. Vane ed.). SPIE Proceedings 834. Society of Photo-Optical Instrumentation Engineers, Bellingham, Washington: 91-105.

Webster, R. 1985. Quantitative spatial analysis of soil in the field. Advances in Soil Science, 3: 1-70.